

Article

Laccase Immobilized Fe₃O₄-Graphene Oxide Nanobiocatalyst Improves Stability and Immobilization Efficiency in the Green Preparation of Sulfa Drugs

Shamila Rouhani ^{1,*}, Shohreh Azizi ^{2,3}, Rose W. Kibechu ⁴, Bhekis B Mamba ^{1,5} and Titus A. M. Msagati ^{1,6} 

¹ Nanotechnology and Water Sustainability Research (NanoWS) Unit, College of Science, Engineering and Technology, University of South Africa, Johannesburg 1709, South Africa; mambabb@unisa.ac.za (B.B.M.); msagatam@unisa.ac.za (T.A.M.M.)

² UNESCO-UNISA Africa Chair in Nanoscience and Nanotechnology College of Graduates Studies, University of South Africa, Muckleneuk Ridge, Pretoria 392, South Africa; azizis@unisa.ac.za

³ Nanosciences African Network (NANOAFNET), iThemba LABS-National Research Foundation, 1 Old Faure Road, Somerset West 7129, Somerset West, Western Cape 722, South Africa

⁴ Department of Chemistry, University of Eswatini, P/Bag 4 Kwaluseni M201, Eswatini; rskibechu@gmail.com

⁵ State Key Laboratory of Separation Membranes and Membrane Process/National Center for International Joint Research on Membrane Science and Technology, Tianjin 300387, China

⁶ School of Life Sciences and Bio-Engineering, The Nelson Mandela African Institution of Science and Technology, Tengeru 447, Arusha, Tanzania

* Correspondence: sh.rouhani78@yahoo.com or rouhas@unisa.ac.za

Received: 11 December 2019; Accepted: 30 December 2019; Published: 23 April 2020



Abstract: This paper, reports on the novel and green synthesis procedure for sulfonamides that involved the immobilization of *Trametes Versicolor* laccase onto the Fe₃O₄-graphene nanocomposite via glutaraldehyde (GA) crosslinking (Lac/Fe₃O₄/GO). Various parameters, mainly, activation time, GA, and laccase concentration were investigated and optimized. The results showed that the optimal contact time was 4 h, GA concentration was 5% while laccase concentration was 5 mg·mL⁻¹, at which a high enzyme activity recovery was achieved (86%). In terms of the stability of immobilized laccase to temperature and storage conditions, the performance of the nanobiocatalyst was found to significantly exceed that of free laccase. The results have indicated that nearly 70% of relative activity for immobilized laccase remained after the incubation period of 2 h at 55 °C, but only 48% of free laccase remained within the same time period. Moreover, the immobilized laccase retained 88% of its initial activity after storage for 20 days. In case of the free laccase, the activity retained within the same time period was 32%. In addition, the nanobiocatalyst possessed better recycling performance as evidenced from the observation that after eight cycles of repeated use, it retained 85% of its original activity.

Keywords: magnetic nanobiocatalyst; immobilization; laccase; Lac/Fe₃O₄/GO; sulfonamides

1. Introduction

Sulfonamide refers to a chemical compound comprised of a sulfonyl group directly bonded to an amine group. Sulfonamide antibiotics or sulfa drugs are normally prescribed to patients suffering from urinary tract infections (UTIs) and other diseases including pneumonia, bronchitis, etc. [1].

Sulfa drugs have also been prescribed to help control seizures and treat diseases and infection including playing a role as HIV protease inhibitors, calcitonin inducers as well as anticancer, antibacterial,

and anti-inflammatory agents [2]. In animal husbandry, sulfonamides are also used as growth promoters in addition to their use as prophylaxis and as antibiotics [3]. The mechanism or mode of action of sulfonamide antibiotics involves the inhibition of the production of dihydrofolic acid in the pathogenic bacteria, which is vital for the production of microbial proteins, and thus interferes with the whole protein synthesis within the microbe leading to the death of microbial cells [1].

In general, sulfa drugs are mostly prepared and produced commercially through a number of synthetic procedures with the most commonly used one employing the reactions of sulfonyl chloride with ammonia or an amine [4–8].

However, these approaches are known to suffer from a number of limitations including the fact that most of these approaches require the presence of transition metals as catalysts, making them more expensive. Moreover, these methods tend to employ toxic solvents as reaction media, which potentially results in the generation of secondary toxicity. Thus, there is a need to investigate and search for other cheaper but safer and efficient approaches for sulfonamide preparation. Lund et al. (2001) and Nematollahi et al. (2014) proposed approaches that involved electrochemical techniques for the preparation of sulfonamides [9,10], which again suffer from low reaction rates and a high-cost, making the method not commercially viable.

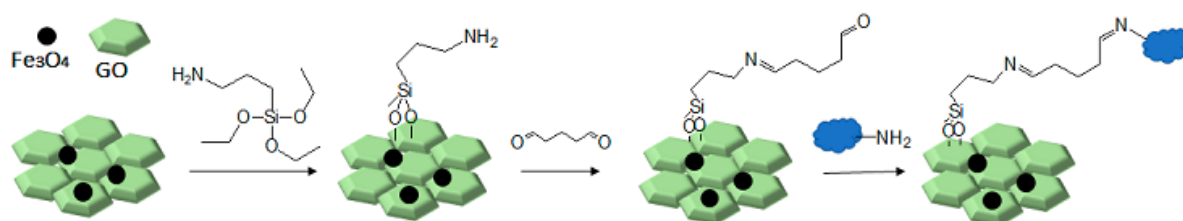
Currently, researchers are working to come up with green and sustainable organic synthesis methods that are safe, cheap, and environmentally friendly. Among such approaches are the enzyme-catalyzed reactions that have of late gained much recognition due to the fact that the reactions involve require only mild conditions to yield high efficiency. Moreover, enzyme-catalyzed reactions are environmentally friendly, not toxic, and generate less by-products [11].

Among the enzymes that have been widely reported in enzyme-catalyzed reactions for the synthesis of many organic compounds, the laccases enzymes belong to a class of oxidases [12]. Each laccase enzyme molecule contains four copper ions, and each of the laccase enzymes carries out one-electron oxidation of an electron-rich aromatic substrate (phenolics and aromatic amines) with the capability to reduce one oxygen molecule to a water molecule [12]. The use of molecular oxygen as an oxidant to produce a water molecule, which is only a by-product, sounds very attractive for catalytic features, thus making laccases one of the best green bio-catalyst in numerous applications [13–17]. However, the use of laccases as a biocatalyst is associated with some limitations as it suffers from low sensitivity, the problem of denaturing agents, and the fact that they are non-reusable, hence not economically viable [18]. The aforementioned challenges for laccases need viable solutions and it is in this idea that some researchers have suggested immobilizing laccases onto carriers in order to play a role as protective agents and also offer the much-needed stability and improved efficiency [17,19–23]. However, the process of immobilizing laccase enzymes onto carriers has also been reported to be accompanied by a significant loss of enzyme activity, which again has prompted scientists and researchers to embark on finding a solution [24–26]. The hope of obtaining solutions to such a problem has received some light due to the discovery of nanostructured composite materials that can provide very suitable immobilization support to render the immobilization process with much needed improved efficiency [27].

One of the nanostructure materials that has received wide recognition is graphene oxide (GO), which is known for its superior properties with a wide range of applications [28–32]. GO is also recognized for its superior morphology, large accessible surface area, richness in terms of oxygenated functional groups, excellent biocompatibility, potential for enhanced functionalization with nanoparticles, and excellent enzyme loading capacity when used as a support. For these reasons, GO has the required qualities to be used as a viable support for enzyme immobilization. Again, GO sheets are associated with undesirable irreversible agglomerates due to the strong π - π interactions, which provide a hindrance for the immobilization process [33]. One solution to such a problem is metallic (magnetic) nanoparticles in either GO or reduced GO nanosheets in order to add to the catalytic effects of GO [34,35]. The attractive features of GO-based magnetic nanocomposites for enzyme immobilization include those related to magnetic response property, easy surface modification,

satisfactory reusability of the magnetic-GO (MGO) two-dimensional structure, simple preparation, large enzyme immobilization capacity, and large surface area [36–38]. Preserving important features of the immobilized catalyst such as stability, loading capacity, and reusability of the immobilized enzymes, surface modification, and reagent coupling are essential due to the fact that direct attachment of the enzyme to MGO nanosheets tends to cause strain to its molecular motion, which also causes the slowing down of its reactivity [39–41].

Therefore, in this work, we report on a novel procedure that involves the functionalization of magnetic graphene oxide ($\text{Fe}_3\text{O}_4/\text{GO}$) with APTES and post-modification with glutaraldehyde, which was used as a spacer. It should be noted that this is a continuation of our previous studies on the preparation and application of magnetically recyclable nanobiocatalysts [42,43]. In this particular work, we report, for the first time, the preparation of the Fe_3O_4 -graphene oxide nanocomposite by a facile in situ co-precipitation method that was successfully utilized as a support for the immobilization of laccase ($\text{Lac}/\text{Fe}_3\text{O}_4/\text{GO}$). Subsequently, it has been employed as a recyclable catalyst for the synthesis of sulfonamide derivatives in good yields via aerobic oxidative coupling of 2,3-dihydrophthalazine-1,4-dione in the presence of sodium benzenesulfonates using air as an oxidant at room temperature (Scheme 1).



Scheme 1. The preparation of $\text{Fe}_3\text{O}_4/\text{GO}$ and its chemical modifications for covalent laccase immobilization.

2. Results and Discussions

2.1. Optimum Conditions for the Preparation of $\text{Lac}/\text{Fe}_3\text{O}_4/\text{GO}$

Figure 1 depicts the optimization results for the activation time, concentration of glutaraldehyde, and laccase immobilization conditions and clearly shows that the concentration of glutaraldehyde increased, with the enhancement of the activity of immobilized laccase up to 65.3 U, 86% (Figure 1a). Beyond this level, the increase in the concentration of GA caused a decline in the activity of the immobilized enzyme (laccase). This was attributed to the fact that the optimal amount of aldehyde groups had been reached at the surface of the magnetic nanocomposite because it is directly linked to the magnitude of the stability of the immobilized enzyme (laccase). When the amount/level of aldehyde groups is high, there is also a tendency of encouraging certain phenomenon including the loss of laccase activity, precipitation, aggregation, and distortion of the enzyme structure [39]. According to Figure 1b, when the activation time was 4 h, the activity of laccase attained the highest level so that the time was now elongated, thus causing the decline in terms of the recovery of laccase which reached 73%, 55.48 U. For this reason, a glutaraldehyde concentration of 5% and activation time of 4 h were chosen as optimal levels for the immobilization of laccase.

In order to investigate the effect of laccase concentration on immobilization, different concentrations of laccase ranging from 1 to 7 ($\text{mg}\cdot\text{mL}^{-1}$) were prepared. Figure 1c shows that the activity of immobilized laccase increased sharply at first from 19 to 65.3 U and then reached a plateau when the initial laccase concentration was higher than $5\text{ mg}\cdot\text{mL}^{-1}$. This may have been caused by saturation of the immobilization sites. Therefore, the optimum initial amount of laccase was chosen as $5\text{ mg}\cdot\text{mL}^{-1}$ for further studies.

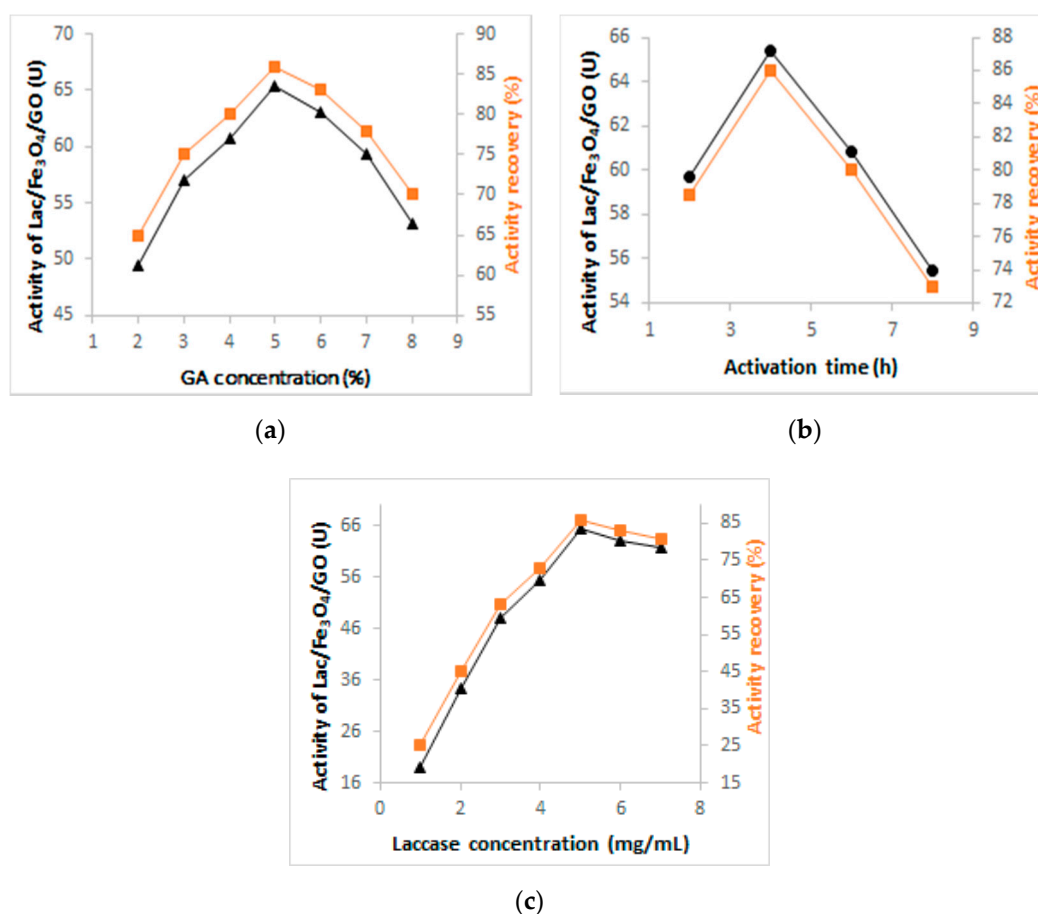


Figure 1. Investigation of the optimum conditions for the preparation of Lac/Fe₃O₄/GO: (a) Effect of GA concentration, (b) activation time and (c) concentration of laccase in the synthesis of Lac/Fe₃O₄/GO.

2.2. Characterization of Lac/Fe₃O₄/GO

Scanning electron microscopy (SEM) was used to investigate the surface morphology of the nanobiocatalyst. The results from the scanning electron micrographs of Fe₃O₄/GO and Lac/Fe₃O₄/GO (Figure 2a,b) confirmed that Fe₃O₄ nanoparticles (A) and the laccase (B) were located on the surface of the GO layers. The average nanoparticle size of the Fe₃O₄/GO and Lac/Fe₃O₄/GO were 28 nm and 63 nm, respectively.

The observations from the x-ray spectroscopy (EDX, Figure 2c) show the presence of the expected elements in the structure of the catalyst, which were oxygen, nitrogen, iron, silicon, and copper in the Lac/Fe₃O₄/GO.

The alternating gradient force magnetometry (AGFM) technique was employed to study the magnetic properties of the Fe₃O₄/GO and Lac/Fe₃O₄/GO. Figure 2d depicts the room temperature magnetization curves of the Fe₃O₄/GO and the Lac/Fe₃O₄/GO where Fe₃O₄/GO and Lac/Fe₃O₄/GO showed the saturation magnetization (M_s) values of 0.002 Oe and 0.003 Oe, respectively. The Fe₃O₄/GO and Lac/Fe₃O₄/GO had a coercivity (H_c) of 27.24 and 8.89 Oe, respectively, and the remanent magnetization (M_r) of ~0.00011 and 0.00048 Oe, respectively. As a result, Lac/Fe₃O₄/GO has a typical superparamagnetic behavior and can be efficiently attracted with an external magnet.

Figure 2e shows the FTIR spectra of GO, Fe₃O₄/GO, NH₂/Fe₃O₄/GO, and GA/Fe₃O₄/GO. The broad peak at 3420 cm⁻¹ represents the O–H stretching bond while peaks at 1728 cm⁻¹ and 1625 cm⁻¹ are the C–O and C=C groups, respectively. The 1060 cm⁻¹ band represents the C–O group of the epoxy functionality [44]. The transmittance signal peak at 590 cm⁻¹ shows the Fe–O resulting from the incorporation of Fe₃O₄ nanoparticles onto a graphene layer. Peaks at 2923 and 2854 cm⁻¹ frequencies represent the result of surface modification by APTES, (NH₂/Fe₃O₄/GO), which also triggered the

symmetric stretching modes of C–H aliphatic peaks from ethylene groups attached to the amino functional groups. The peaks at 692 and 1583 cm^{-1} represent the presence of the N–H [45]. The peak signals at 1236 and 1041 cm^{-1} corresponded to Si–O–Si and Si–O–C [46]. The broad intense peak around 3420 cm^{-1} was for the OH groups. The OH group was found to decrease, due to the fact that amino-silylation might have taken place via reaction with the hydroxyl groups present at the surface. A band at 1633 cm^{-1} represented the nitrile functional group ($-\text{C}=\text{N}-$), which resulted from the reaction between the free amino groups of $\text{NH}_2/\text{Fe}_3\text{O}_4/\text{GO}$ and $-\text{CHO}$ of the glutaraldehyde. Therefore, from the results shown in Figure 2e, the connection between $\text{NH}_2/\text{Fe}_3\text{O}_4/\text{GO}$ and laccase was successfully established using the cross-linker glutaraldehyde.

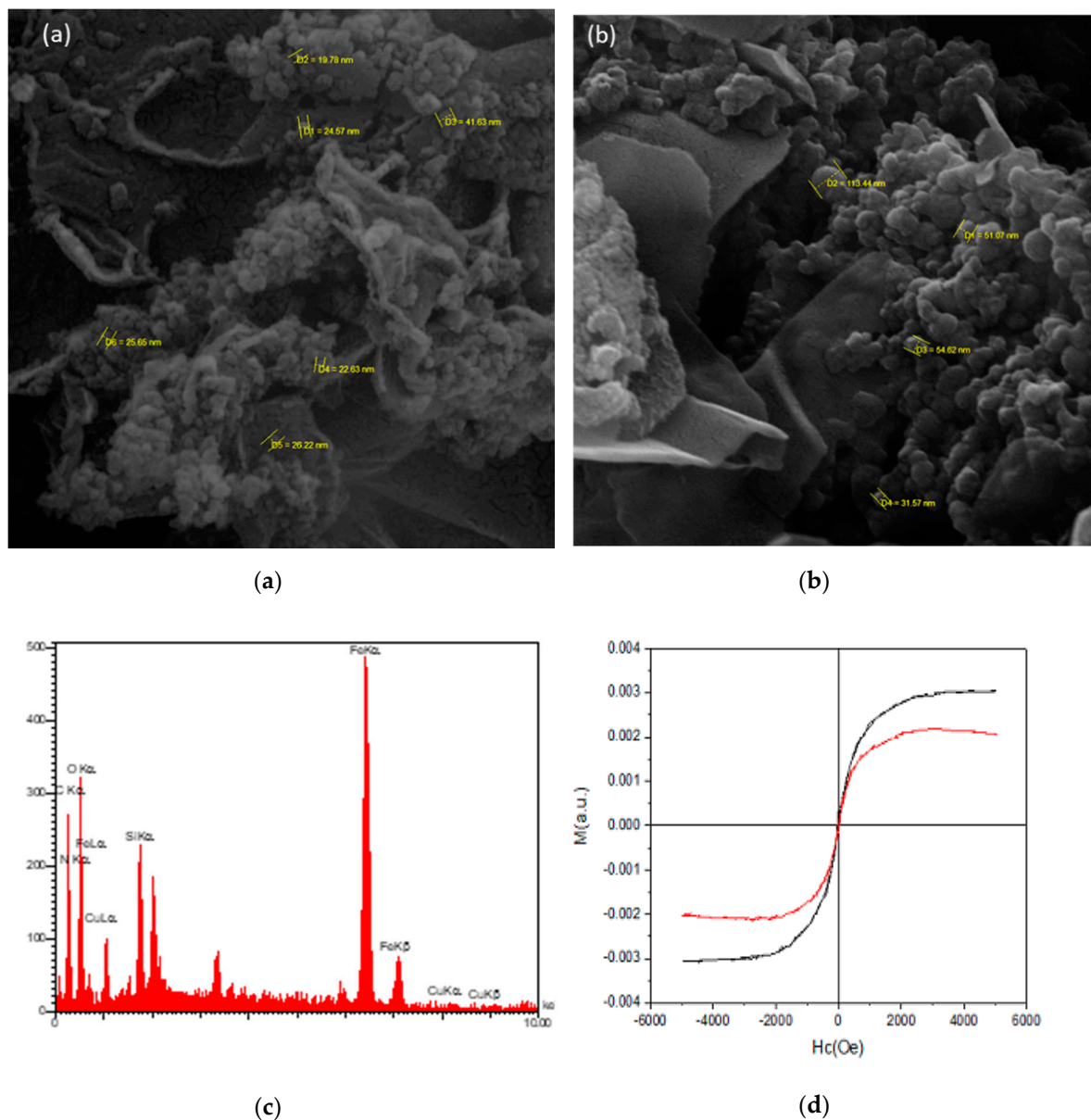
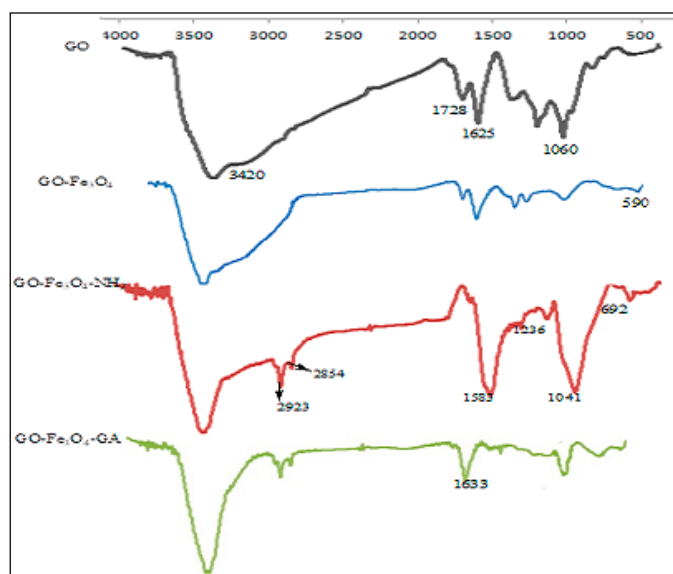


Figure 2. Cont.



(e)

Figure 2. SEM micrographs of (a) $\text{Fe}_3\text{O}_4/\text{GO}$ and (b) $\text{Lac}/\text{Fe}_3\text{O}_4/\text{GO}$. (c) EDX spectrum of $\text{Lac}/\text{Fe}_3\text{O}_4/\text{GO}$. (d) Magnetic curves of $\text{Fe}_3\text{O}_4/\text{GO}$ and $\text{Lac}/\text{Fe}_3\text{O}_4/\text{GO}$ at room temperature. (e) FT-IR spectra of GO , $\text{Fe}_3\text{O}_4/\text{GO}$, $\text{NH}_2/\text{Fe}_3\text{O}_4/\text{GO}$, $\text{GA}/\text{Fe}_3\text{O}_4/\text{GO}$.

2.3. Investigation of the Activity and Characteristic Properties of Free Laccase and $\text{Lac}/\text{Fe}_3\text{O}_4/\text{GO}$

2.3.1. Estimation of Kinetic Parameters for the Free Enzyme Laccase and $\text{Lac}/\text{Fe}_3\text{O}_4/\text{GO}$

The investigation of the kinetic parameters for the activity of free laccase and $\text{Lac}/\text{Fe}_3\text{O}_4/\text{GO}$ was performed using the approach given in Table 1. The results showed that the K_m values for the free laccase increased from 0.045 mM to 0.073 mM after the immobilization. As for V_{\max} , a value of 2.9 mM min^{-1} was recorded for the free laccase, which decreased 1.4 mM min^{-1} upon immobilization. This trend, which resulted in the increase of K_m and decrease of V_{\max} after the immobilization, might have been caused by the steric hindrances on the active site of the enzyme caused by the introduction of the support [47].

Table 1. Parameters investigated for free laccase and $\text{Lac}/\text{Fe}_3\text{O}_4/\text{GO}$.

Entry	Enzyme	$K_m[\text{mM}]$	V_{\max}
1	Free Laccase	0.045	2.9
2	$\text{Lac}/\text{Fe}_3\text{O}_4/\text{GO}$	0.073	1.4

2.3.2. Effect of Temperature and pH on the Activity of Free and Immobilized Laccase

Figure 3a shows the results of the investigation of the dependence of pH on the activity of both the free as well as immobilized enzymes, which was performed within the pH range of pH 3–pH 8 at room temperature while setting the highest activity at 100%. Immobilization of enzymes onto charged supports is normally the reason for the deviations of the pH-activity profile to either high or low pH regions [46,47]. The results from this study have indicated that there was no difference in terms of the profile of pH-activity between the free and the immobilized laccase at an optimum pH of 5, although the immobilized laccase showed better adaptability in a wider pH region compared to the free laccase. It was also observed that the immobilization did not significantly alter the enzyme's catalytic performance. The results from this study also found that $\text{Lac}/\text{Fe}_3\text{O}_4/\text{GO}$ retained almost 65% activity at pH 3, while free laccase retained about 40% activity at the same pH. When pH was changed

to 8.0, the activities of Lac/Fe₃O₄/GO retained more than 60% after 2 h while the free laccase retained 25.3% activity at the same time period.

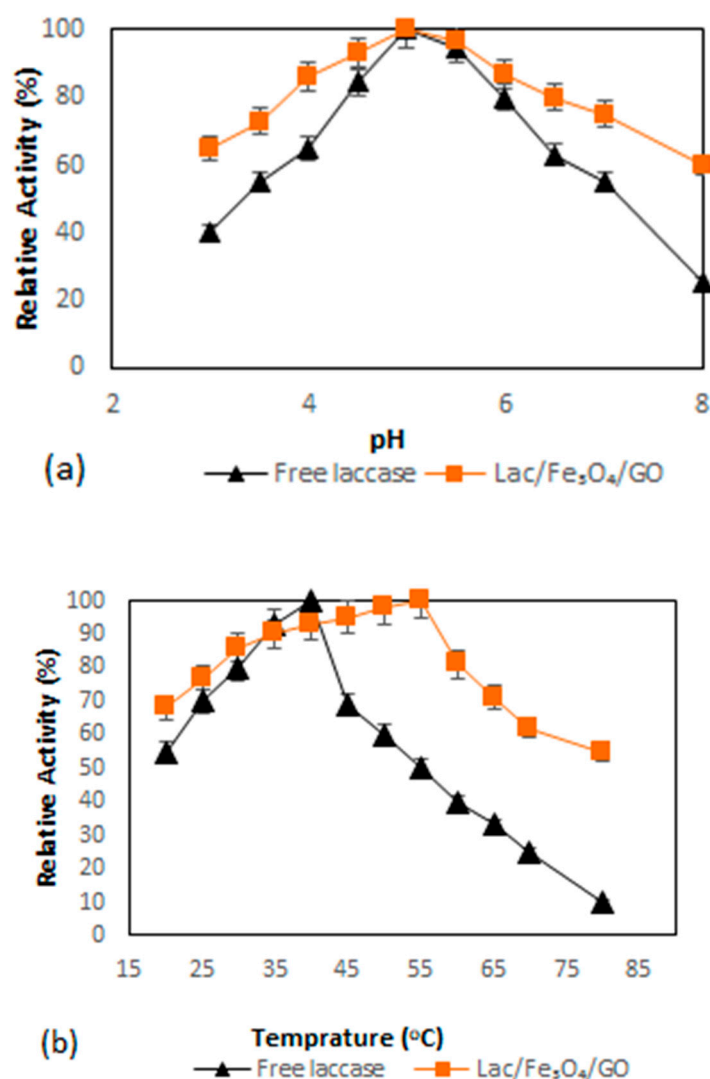


Figure 3. (a) Effect of pH on the activity of the free laccase and Lac/Fe₃O₄/GO (Na-acetate buffer for pH = 3–5 and Na-phosphate buffer for pH = 6–8) by the ABTS aerobic oxidation reaction at room temperature for two hours. (b) Effect of temperature on free laccase and Lac/Fe₃O₄/GO. The relative activity was determined at various temperatures at pH = 5 by ABTS aerobic oxidation reaction. All experiments were performed in triplicate. The error bars were determined (5%).

The effect of temperature on the activities of laccase in this work was investigated by monitoring its effect on the enzyme activity by varying temperature from 20 °C to 80 °C (Figure 3b). The maximum activity of free laccase was found to be 40 °C, while that of Lac/Fe₃O₄/GO was recorded at 55 °C. The activity of free laccase was observed to decrease sharply at temperatures above 40 °C, while in the case of Lac/Fe₃O₄/GO, a broader temperature for optimum activity was observed at temperatures ranging from 40 to 60 °C, with 19% loss inactivity. When the temperature was raised to 70 °C, the Lac/Fe₃O₄/GO still retained more than 62% activity, while at the same temperature, the free laccase retained 25% activity. This trend may be caused by the enhanced structural stability of Lac/Fe₃O₄/GO resulting from the presence of multi-layer graphene oxide-enzyme nanosheets, while the multipoint covalent interactions between the laccase molecules and functionalized graphene oxide-Fe₃O₄ nanocomposite, which may have rendered additional protection against possible inactivation at such elevated temperature and pH changes [48].

2.3.3. Thermal and Storage Stability

The investigation of the heat inactivation was performed in order to evaluate the effect of Fe_3O_4 -graphene oxide nanocomposite on the thermal stability of laccase enzymes. The immobilized and free laccase were incubated at different temperatures ranging between 15–85 °C for two hours and subsequently assayed for residual activity. Figure 4a depicts the results whereby after two hours of incubation, the immobilized and free laccase showed a decreasing trend of relative activity with further temperature increases. Moreover, it was further revealed that the enzymatic activity of free laccase declined sharply after incubation at 55 °C and lost approximately 50% of its activity after 2 h. In contrast, more than 70% of the enzymatic activity of immobilized laccase remained after the same time period. The relative activity of Lac/ Fe_3O_4 /GO was found to decrease at a slower rate than that of the free one at a higher temperature (40–60 °C). The main factor responsible for this improvement in thermostability might be the covalent interactions between the multi-layer magnetic graphene oxide nanosheet and laccase, which can decrease enzyme mobility and the conformational changes; thus, causing increased stability against the effects of thermal denaturation.

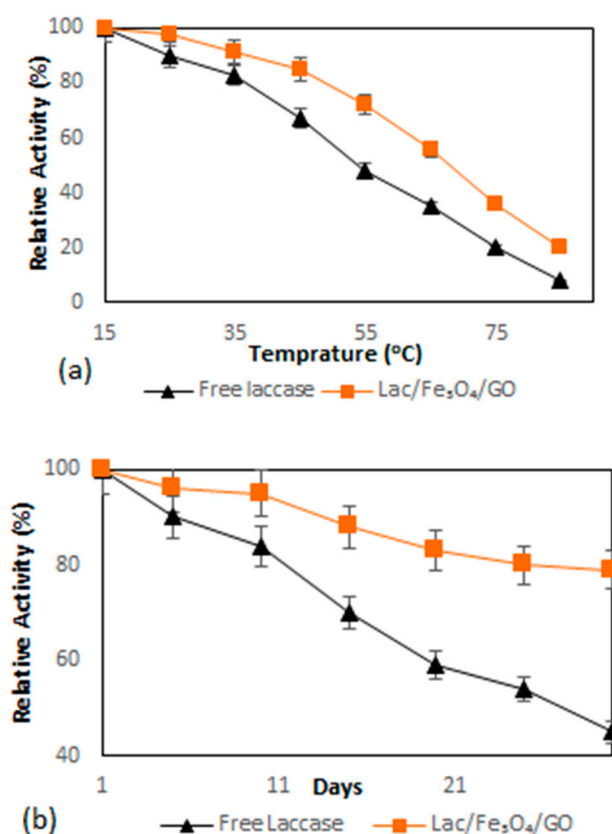


Figure 4. (a) Thermal stability of free laccase and Lac/ Fe_3O_4 /GO determined at different temperatures (15–85 °C) in PBS solution (0.1 M, pH = 5) by the ABTS aerobic oxidation reaction for two hours. (b) Storage stability of free laccase and Lac/ Fe_3O_4 /GO in PBS solution (0.1 M, pH = 5) determined by the ABTS aerobic oxidation reaction at 4 °C. Experiments were performed in triplicate. The error bars were determined (5%).

The stability of laccase during storage was worked-out by computing the relative activity in PBS buffer (0.1 M, pH = 5) at 4 °C while setting the initial laccase activity at 100%. The results of the study on the stability of the enzyme are depicted in Figure 4b, where it shows that after 20 days of storage, the Lac/Fe₃O₄/GO retained 88% of its original activity. In the case of the free laccase, only about 40% of its original activity was retained. The results further indicate that Lac/Fe₃O₄/GO is capable of improving the storage stability of the biocatalyst because it can restrict enzyme conformational changes [49,50]. For this reason, it can be concluded that the enhanced storage stability of Lac/Fe₃O₄/GO could prove to be of significant importance in cutting the costs for industrial applications.

2.4. The Catalytic Application of Lac/Fe₃O₄/GO in the Aerobic Oxidative Coupling of 2,3-Dihydrophthalazine-1,4-dione and Sodium Benzenesulfinates at Mild Conditions

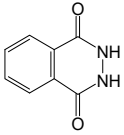
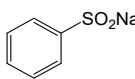
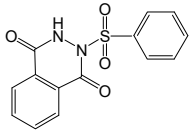
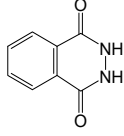
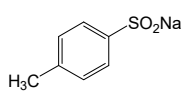
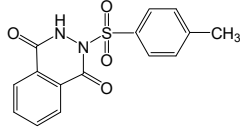
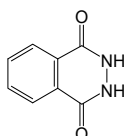
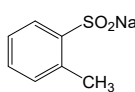
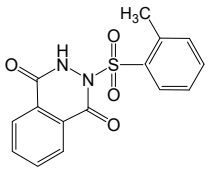
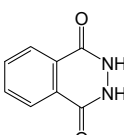
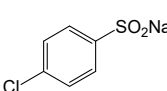
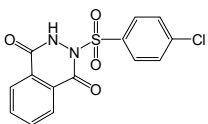
The catalytic activity of Lac/Fe₃O₄/GO as a recoverable nanobiocatalyst was investigated for the synthesis of sulfonamides in PBS solution at ambient temperature. The optimization of the reaction conditions for the synthesis of sulfonamides took into account the influence of the nanobiocatalyst as well as the type of solvent on the product yield in the equimolar reactions of phthalhydrazide and p-toluene sulfinic sodium salt, which were studied at room temperature (Table 2). The results also indicate that the reaction could not take place without the presence of Lac/Fe₃O₄/GO and in its absence, even after 24 h (Table 2), no reaction could take place. The observations from this study indicate that when Fe₃O₄ was used as a catalyst instead of Lac/Fe₃O₄/GO under the same reaction conditions, a yield of 10% for a corresponding sulfonamide was obtained (Table 2). Moreover, Lac/Fe₃O₄/GO (50 U) in the PBS buffer (0.1 M, pH = 6) was found to be an optimum amount that is ideal for the synthesis of 2-(phenylsulfonyl)-2,3-dihydrophthalazine-1,4-dione. In this work, the reactions were performed in various solvents to investigate the effects of the solvents. The results from this work have shown that the most effective solvent was PBS (pH = 5, 0.1 M). In H₂O, EtOH, and H₂O:EtOH (1:1) where the reactions gave yields, the results ranged between 40% to 60% (Table 2). Some solvents such as DMF and DMSO gave no reaction, presumably due to the denaturation of the laccase enzyme.

Table 2. Optimization experiments to investigate the effect of the catalyst and solvent on the synthesis of 2-(phenylsulfonyl)-2,3-dihydrophthalazine-1,4-dione.

Entry	Catalyst (U)	Solvent	GC Yield (%)
1	No Lac/Fe ₃ O ₄ /GO	PBS (0.1 M pH = 5)	–
2	Fe ₃ O ₄ (50 mg)	PBS (0.1 M pH = 5)	10
3	Lac/Fe ₃ O ₄ /GO (30)	PBS (0.1 M pH = 5)	34
4	Lac/Fe ₃ O ₄ /GO (40)	PBS (0.1 M pH = 5)	75
5	Lac/Fe ₃ O ₄ /GO (50)	PBS (0.1 M pH = 5)	>99
6	Lac/Fe ₃ O ₄ /GO (50)	PBS (0.1 M pH = 4)	80
7	Lac/Fe ₃ O ₄ /GO (50)	PBS (0.1 M pH = 6)	85
8	Lac/Fe ₃ O ₄ /GO (50)	PBS (0.1 M pH = 7)	67
9	Lac/Fe ₃ O ₄ /GO (50)	0.1 M sodium acetate buffer pH = 5	70
10	Lac/Fe ₃ O ₄ /GO (50)	H ₂ O	40
11	Lac/Fe ₃ O ₄ /GO (50)	EtOH	53
12	Lac/Fe ₃ O ₄ /GO (50)	H ₂ O/EtOH (1:1)	60
13	Lac/Fe ₃ O ₄ /GO (50)	DMSO	–
14	Lac/Fe ₃ O ₄ /GO (50)	DMF	–

In order to generalize the scope of the reaction, 2,3-dihydrophthalazine-1,4-dione with sodium benzenesulfinates derivatives were examined under optimal conditions, and the results are listed in Table 3.

Table 3. Synthesis of sulfonamide derivatives in the presence of Lac/Fe₃O₄/GO and aerial oxygen at room temperature.

Entry	2,3-dihydrophthalazine-1,4-dione	Sodium Benzenesulfinate	Product	Yield (%)
1				81
2				95
3				90
4				73

2.5. Reusability of Lac/Fe₃O₄/GO

The recovery and reusability of Lac/Fe₃O₄/GO were investigated for the synthesis of 2-(phenylsulfonyl)-2,3-dihydrophthalazine-1,4-dione via aerobic oxidative coupling of 2,3-dihydrophthalazine-1,4-dione and p-toluene sulfinic sodium salt. It took at least 24 h for the Lac/Fe₃O₄/GO to separate from the mixture through the influence of an external magnet. The results show that 85% of the initial activity of the recycled enzyme was retained after eight consecutive reaction runs (Figure 5). The cause for the loss of activity could be due to either the leakage of the enzyme from the support's surface, or its inactivation as a result of the enzymatic conformational changes that might have taken place during the storage phase.

**Figure 5.** Recycling experiment of Lac/Fe₃O₄/GO for oxidative coupling between 2,3-dihydrophthalazine-1,4-dione and p-toluene sulfinic sodium salt in the presence of aerial oxygen and in the phosphate buffer solution (PBS) (0.1 M, pH = 5) at room temperature for 24 h.

3. Methods

3.1. Chemicals

Laccase (E.C. 1.10.3.2) from *Trametes Versicolor*, 2,2-azinobis(3-ethylbenzthiazolin-6-sulfonate) (ABTS), 3-aminopropyltriethoxysilane (APTES), glutaraldehyde (GA), iron(II) chloride tetrahydrate ($\text{FeCl}_2 \cdot 4\text{H}_2\text{O}$), iron(III) chloride hexahydrate ($\text{FeCl}_3 \cdot 6\text{H}_2\text{O}$), ammoniumhydroxide (25%, *w/w*), graphite, potassium permanganate (KMnO_4), concentrated sulfuric acid (H_2SO_4), sodium nitrate, sodium hydroxide, hydrogen peroxide, (30% *w/w*), toluene, and ethanol were purchased from Sigma-Aldrich Co. LLC. (St. Louis, CA, USA). All other materials were also bought from Sigma and used without any additional purification.

3.2. Preparation of Graphene Oxide

Graphene oxide (GO) was prepared using the modified Hummers method [44]. Graphite (3 g) was added into concentrated sulfuric acid (150 mL) under continuous stirring in ice water then sodium nitrate (3 g) was added while stirring. The potassium permanganate (KMnO_4) (18 g) was slowly added into the reaction and stirred for 2 h. Then, the reaction was heated to 35 °C and stirred for a further 30 min. The distilled water (200 mL) was then added to the reaction mixture and the temperature was again increased to 90 °C and maintained for 20 min. The reaction mixture was then cooled down to room temperature. Then, hydrogen peroxide (18 mL) was added in order to neutralize the unused KMnO_4 . This resulted in the formation of a bright yellow solution and a precipitate was formed and collected by centrifugation. The precipitate was washed several times using hydrochloric acid (5% *v/v*) before being washed with distilled water until the pH of the supernatant reached neutral levels. Finally, the obtained sample was dried in a vacuum oven at 60 °C overnight.

3.3. Preparation of $\text{Fe}_3\text{O}_4/\text{GO}$ Nanocomposite

Fe_3O_4 nanoparticles were deposited over the surface of graphene oxide by a co-precipitation method based on the hydrolysis of a mixture of Fe^{2+} and Fe^{3+} ions (molar ratio 1:2). Initially, the GO (3 g) was dispersed in distilled water (150 mL) by sonication for 1 h. A solution of $\text{FeCl}_3 \cdot 6\text{H}_2\text{O}$ (3 g) and $\text{FeCl}_2 \cdot 4\text{H}_2\text{O}$ (1.10 g) in distilled water (100 mL) was then added dropwise to the suspension and mechanically stirred for 30 min under nitrogen at room temperature. The temperature of the mixture was then increased to 80 °C and the NH_4OH solution (60 mL; 25%) was added dropwise until the pH reached about pH 11. After 60 min, the temperature was decreased and the resulting precipitate was filtered, washed, and dried at 50 °C for 12 h to obtain $\text{Fe}_3\text{O}_4/\text{GO}$.

3.4. Preparation of $\text{NH}_2/\text{Fe}_3\text{O}_4/\text{GO}$, $\text{GA}/\text{Fe}_3\text{O}_4/\text{GO}$, and Immobilization of Laccase onto $\text{Fe}_3\text{O}_4/\text{GO}$ Nanocomposite

In order to introduce the much needed appropriate functional groups onto the $\text{Fe}_3\text{O}_4/\text{GO}$, surface modification had to be performed. This was carried out by treating $\text{Fe}_3\text{O}_4/\text{GO}$ with APTES to introduce amine groups. The surface modification procedures were initiated by adding $\text{Fe}_3\text{O}_4/\text{GO}$ nanocomposites (3 g) to the anhydrous toluene (60 mL), followed by APTES (60 mL). The solution was then refluxed at 80 °C for 12 h. The resulting product was separated by an external magnetic field using a magnet and washed several times with ethanol and dried in a vacuum oven at 60 °C overnight. Then, the $\text{NH}_2/\text{Fe}_3\text{O}_4/\text{GO}$ was sonicated in PBS buffer (60 mL; 0.1 M pH = 7) for two hours, and then crosslinked with glutaraldehyde (under the optimal GA concentration) at 25 °C while stirring at different times (i.e., 2, 4, 6, and 8 h). The concentration of glutaraldehyde solution was set from 2% to 8%. Then, the excess glutaraldehyde was washed with PBS buffer in the presence of an external magnet and $\text{GA}/\text{Fe}_3\text{O}_4/\text{GO}$ was the resulting aldehyde containing product.

In order to immobilize the laccase $\text{GA}/\text{Fe}_3\text{O}_4/\text{GO}$ solution in PBS solution (0.1 M pH = 5), it was ultrasonicated for 30 min and mixed with a solution of laccase (5 mL) in PBS solution (0.1 M pH = 5) with the optimal laccase concentration (15.2 U, 5 $\text{mg} \cdot \text{mL}^{-1}$) and the reaction mixture was shaken at 4 °C for 24 h. The concentration of laccase solution was set from 1 to 7 $\text{mg} \cdot \text{mL}^{-1}$. Then, the immobilized

laccase was separated using a magnet, before being washed with PBS solution (0.1 M pH = 5). The washing process was repeated several times until no free laccase was detected in the rinsing solution. The residual concentration of laccase in the rinsing solution was determined by the Bradford method [51]. The product was then dried under reduced pressure and stored at 4 °C for future use.

3.5. Activity Assay of Free and Immobilized Laccase

The activities of free and immobilized laccase were measured using ABTS as a standard in Na-acetate buffer (0.1 M, pH = 5.0) as described previously [52].

3.6. Determination of Kinetic Parameters of Free and Immobilized Laccase

The Michaelis–Menten constant (K_m) and apparent maximum velocity (V_{max}) were determined with varying concentrations of ABTS (0.01–1 mM) in PBS solution (0.1 M pH = 5) at 25 °C. The kinetic parameter values for the substrate (ABTS) were obtained according to the Lineweaver–Burk plot and K_m and V_{max} were determined from the intercepts at x and y axes, respectively.

3.7. Effect of Temperature and pH on the Activity of Free and Immobilized Laccase

The effect of pH on the activity of free and immobilized laccase was determined at a pH range between 3 to 8 at room temperature for two hours using the standard ABTS assay. The buffers used were Na-acetate buffer for pH = 3–5 and Na-phosphate buffer for pH = 6–8. The effect of temperature on the biocatalyst activity was assayed at different temperatures ranging from 20 to 80 °C in PBS solution at pH = 5. Laccase activity was determined using the standard ABTS assay. Relative activities were normalized to the highest activity, which was taken as 100%.

3.8. Thermal and Storage Stability of Free and Immobilized Laccase

Thermal stability was investigated by incubating the free and immobilized laccase at different temperatures ranging from 15 to 85 °C in PBS solution (0.1 M, pH = 5) for 2 h; thereafter, the residual enzymatic activity was measured using the standard ABTS assay. Storage stability of the free and immobilized laccase was ensured upon calculating the residual activity of immobilized and free laccase using the standard ABTS assay after being stored at 4 °C in PBS solution (0.1 M, pH = 5) for 20 days. In all stability experiments, the initial activity of the immobilized laccase was assumed as 100%, while other activities were the relative values in comparison with the initial activity.

3.9. General Procedure for Synthesis of Sulfonamide Derivatives by Aerobic Oxidative Coupling between 2,3-Dihydrophthalazine-1,4-Dione and Sodium Benzenesulfonates in the Presence of Lac/Fe₃O₄/GO as a Recoverable Nanobiocatalyst

Sodium benzenesulfonates (1 mmol) was added to a mixture of Lac/Fe₃O₄/GO (50 U) and 2,3-dihydrophthalazine-1,4-dione (1 mmol) in PBS buffer (15 mL; 0.1 M pH = 5). Then, the reaction was stirred under air at room temperature for 24 h. The catalyst was separated by an external magnet and the solid was collected by suction filtration and washed, dried, and then characterized using various techniques including FTIR and NMR (¹H and ¹³C) (See Supplementary Material).

4. Conclusions

In the present study, *Trametes Versicolor* laccase was successfully immobilized onto an Fe₃O₄-graphene oxide nanocomposite using glutaraldehyde as a cross-linking reagent and then characterized by various techniques. The optimum conditions for laccase immobilization on the functionalized Fe₃O₄/GO were determined. Compared to free laccase, the stability of Lac/Fe₃O₄/GO was based on the ability of thermal tolerance, pH, and long-term storage, where it was observed that for Lac/Fe₃O₄/GO, there was an improvement of up to 37%, 25%, and 48%, respectively. For the first time tolerance, Lac/Fe₃O₄/GO was used as a highly active and efficient nanobiocatalyst for the synthesis of sulfonamides in good yields through the oxidative coupling of 2,3-dihydrophthalazine-1,4-dione with

sodium benzene sulfonates in PBS (0.1 M, pH = 5) as a green solvent and using air as an oxidant at room temperature. The nanobiocatalyst was also found to have both (i) heterogeneous catalysis advantages, and significantly high reusability without any significant loss of activity) and (ii) homogeneous free laccase properties, which positioned it as a very reliable alternative for applications related to the synthesis of sulfa drugs.

Supplementary Materials: The following are available online at <http://www.mdpi.com/2073-4344/10/4/459/s1>, Spectral data of some synthesized compounds.

Author Contributions: Conceptualization, S.R.; Methodology, S.A.; Investigation, S.R.; Writing—original draft preparation, S.R.; Writing—review and editing, R.W.K. and B.B.M.; Supervision, T.A.M.M. All authors have read and agreed to the published version of the manuscript.

Funding: This research received no external funding.

Acknowledgments: We are grateful to the University of South Africa (NanoWS Research Unit) for their partial support of this work.

Conflicts of Interest: The authors declare no conflicts of interest.

References

1. Henry, R.J. The Mode of Action of Sulfonamides. *Bacteriol. Rev.* **1943**, *7*, 175–262. [[CrossRef](#)]
2. Ganguly, A.K.; Alluri, S.S.; Carocchia, D.; Biswas, D.; Wang, C.H.; Kang, E.; Zhang, Y.; McPhail, A.T.; Carroll, S.S.; Burlein, C.; et al. Design, synthesis, and X-ray crystallographic analysis of a novel class of HIV-1 protease inhibitors. *J. Med. Chem.* **2011**, *54*, 7176–7183. [[CrossRef](#)]
3. Msagati, T.A.M.; Nindi, M.M. Multiresidue determination of sulfonamides in a variety of biological matrices by supported liquid membrane with high pressure liquid chromatography-electrospray mass spectrometry detection. *Talanta* **2004**, *64*, 87–100. [[CrossRef](#)]
4. Shi, F.M.; Tse, K.X.; Cui, J.; Gordes, D.; Michalik, D.; Thurow, K.; Deng, Y.Q.; Beller, M. Copper-catalyzed alkylation of sulfonamides with alcohols. *Angew. Chem. Int. Ed.* **2009**, *48*, 5912–5915. [[CrossRef](#)] [[PubMed](#)]
5. Huang, X.; Wang, J.C.; Ni, Z.Q.; Wang, S.C.; Pan, Y.J. Copper-mediated S–N formation via an oxygen-activated radical process: A new synthesis method for sulphonamides. *Chem. Commun.* **2014**, *50*, 4582–4584. [[CrossRef](#)]
6. Pan, X.; Gao, J.; Liu, J.; Lai, J.; Jiang, H.; Yuan, G. Synthesis of sulfonamides via I₂-mediated reaction of sodium sulfinates with amines in an aqueous medium at room temperature. *Green Chem.* **2015**, *17*, 1400–1403. [[CrossRef](#)]
7. Rosen, B.R.; Ruble, J.C.; Beauchamp, T.J.; Navarro, A. Mild Pd-Catalyzed N-Arylation of Methanesulfonamide and Related Nucleophiles: Avoiding Potentially Genotoxic Reagents and Byproducts. *Org. Lett.* **2011**, *13*, 2564–2567. [[CrossRef](#)] [[PubMed](#)]
8. Tang, X.D.; Huang, L.B.; Qi, C.R.; Wu, X.; Wu, W.Q.; Jiang, H.F. Copper-catalyzed sulfonamides formation from sodium sulfinates and amines. *Chem. Commun.* **2013**, *49*, 6102–6104. [[CrossRef](#)] [[PubMed](#)]
9. Nematollahi, D.; Hosseiny Davarani, S.S.; Mirahmadpour, P.; Varmaghani, F. A facile electrochemical method for the synthesis of new sulfonamide derivatives of potential biological significance. *Chin. Chem. Lett.* **2014**, *25*, 593–595. [[CrossRef](#)]
10. Lund, H.; Hammerich, O. *Organic Electrochemistry*, 4th ed.; Marcel Dekker Inc.: New York, NY, USA, 2001.
11. Garcia, J.; Zhang, Y.; Taylor, H.; Cespedes, O.; Webb, M.E.; Zhou, D.J. Multilayer enzyme-coupled magnetic nanoparticles as efficient, reusable biocatalysts and biosensors. *Nanoscale* **2011**, *3*, 3721–3730. [[CrossRef](#)]
12. Couto, S.; Toco-Herrera, J.L. Industrial and biotechnological applications of laccases: A review. *Biotechnol. Adv.* **2006**, *24*, 500–513. [[CrossRef](#)]
13. Riva, S. Laccases: Blue enzyme for green chemistry. *Trends Biotechnol.* **2006**, *24*, 219–226. [[CrossRef](#)]
14. Viswanath, B.; Rajesh, B.; Janardhan, A.; Kumar, A.P.; Narasimha, G. Fungal laccases and their applications in bioremediation. *Enzyme Res.* **2014**, *2014*, 1. [[CrossRef](#)] [[PubMed](#)]
15. Pezzella, C.; Guarino, L.; Piscitelli, A. How to enjoy laccases. *Cell. Mol. Life Sci.* **2015**, *72*, 923–940. [[CrossRef](#)]
16. Kudanga, T.; Roes-Hill, M.L. Laccase applications in biofuels production: Current status and future prospects. *Appl. Microbiol. Biotechnol.* **2014**, *98*, 6525–6542. [[CrossRef](#)] [[PubMed](#)]
17. Yang, J.; Li, W.; Ng, T.B.; Deng, X.; Lin, J.; Ye, X. Laccases: Production, expression regulation, and applications in pharmaceutical biodegradation. *Front. Microbiol.* **2017**, *8*, 832. [[CrossRef](#)] [[PubMed](#)]

18. Stanescu, M.D.; Fogorasi, M.; Shaskolskiv, B.L.; Gavrilas, S.; Lozinsky, V.I. New Potential Biocatalysts by Laccase Immobilization in PVA Cryogel Type Carrier. *Appl. Biochem. Biotechnol.* **2010**, *160*, 1947–1954. [[CrossRef](#)]
19. Kulys, J.; Vidziunaite, R.; Schneider, P. Laccase-catalyzed oxidation of naphthol in the presence of soluble polymers. *Enzyme Microb. Technol.* **2003**, *32*, 455–463. [[CrossRef](#)]
20. Saoudi, O.; Ghaouar, N.; Bensalah, S.; Othman, T. Denaturation process of laccase in various media by refractive index measurements. *Biochem. Biophys. Rep.* **2017**, *11*, 19–26. [[CrossRef](#)]
21. Nasoohi, N.; Khajeh, K.; Mohammadian, M.; Ranjbar, B. Enhancement of catalysis and functional expression of a bacterial laccase by single amino acid replacement. *Int. J. Biol. Macromol.* **2013**, *60*, 56–61. [[CrossRef](#)]
22. Abejon, R.; Belleville, M.P.; Marcano, J.S. Design, economic evaluation and optimization of enzymatic membrane reactors for antibiotics degradation in wastewaters. *Sep. Purif. Technol.* **2015**, *156*, 183–199. [[CrossRef](#)]
23. Tran, D.N.; Balkus, K.J. Perspective of recent progress in immobilization of enzymes. *ACS Catal.* **2011**, *1*, 956–968. [[CrossRef](#)]
24. Singh, R.K.; Tiwari, M.K.; Singh, R.; Haw, J.R.; Lee, J.K. Immobilization of Larabinitol dehydrogenase on aldehyde-functionalized silicon oxide nanoparticles for Lxylulose production. *Appl. Microbiol. Biotechnol.* **2014**, *98*, 1095–1104. [[CrossRef](#)] [[PubMed](#)]
25. Zhang, Y.; Ge, J.; Liu, Z. Enhanced activity of immobilized or chemically modified enzymes. *ACS Catal.* **2015**, *5*, 4503–4513. [[CrossRef](#)]
26. Zhang, Y.; Zhang, J.; Huang, X.; Zhou, X.; Wu, H.; Guo, S. Assembly of graphene oxide–enzyme conjugates through hydrophobic interaction. *Small* **2012**, *8*, 154–159. [[CrossRef](#)] [[PubMed](#)]
27. Gao, Z.; Zharov, I. Large pore mesoporous silica nanoparticles by templating with a nonsurfactant molecule, tannic acid. *Chem. Mater.* **2014**, *26*, 2030–2037. [[CrossRef](#)]
28. Geim, K.; Novoselov, K.S. The rise of graphene. *Nat. Mater.* **2007**, *6*, 183–191. [[CrossRef](#)]
29. Singh, V.; Joung, D.; Zhai, L.; Das, S.; Khondaker, S.; Seal, S. Graphene based materials: Past, present and future. *Prog. Mater. Sci.* **2011**, *56*, 1178–1271. [[CrossRef](#)]
30. Bi, H.; Xie, X.; Yin, K.; Zhou, Y.; Wan, S.; He, L.; Xu, F.; Banhart, F.; Sun, L.; Ruoff, R.S. Spongy Graphene as a Highly Efficient and Recyclable Sorbent for Oils and Organic Solvents. *Adv. Funct. Mater.* **2012**, *22*, 4421–4425. [[CrossRef](#)]
31. Huang, X.; Yin, Z.; Wu, S.; Qi, X.; He, Q.; Zhang, Q.; Yan, Q.; Boey, F.; Zhang, H. Graphene-based materials: Synthesis, characterization, properties, and applications. *Small* **2011**, *7*, 1876–1902. [[CrossRef](#)]
32. Xu, W.; Ling, X.; Xiao, J.; Dresselhaus, M.; Kong, J.; Xu, H.; Liu, Z.; Zhang, J. Surface enhanced Raman spectroscopy on a flat graphene surface. *Proc. Natl. Acad. Sci. USA* **2012**, *109*, 9281–9286. [[CrossRef](#)] [[PubMed](#)]
33. Li, J.; Zhang, S.; Chen, C.; Zhao, G.; Yang, X.; Li, J.; Wang, X. Removal of Cu (II) and fulvic acid by graphene oxide nanosheets decorated with Fe₃O₄ nanoparticles. *ACS Appl. Mater. Interfaces* **2012**, *4*, 4991–5000. [[CrossRef](#)] [[PubMed](#)]
34. Kotan, G.; Kardaş, F.; Yokuş, Ö.A.; Akyıldırım, O.; Saral, H.; Eren, T.; Yola, M.L.; Atar, N. A novel determination of curcumin via Ru@ Au nanoparticle decorated nitrogen and sulfur-functionalized reduced graphene oxide nanomaterials. *Anal. Methods* **2016**, *8*, 401–408. [[CrossRef](#)]
35. Akyıldırım, O.; Yüksek, H.; Saral, H.; Ermiş, İ.; Eren, T.; Yola, M.L. Platinum nanoparticles supported on nitrogen and sulfur-doped reduced graphene oxide nanomaterial as highly active electrocatalysts for methanol oxidation. *J. Mater. Sci. Mater. Electron.* **2016**, *27*, 8559–8566. [[CrossRef](#)]
36. Xu, C.; Wang, X.; Zhu, J.; Yang, X.; Lu, L. Deposition of Co₃O₄ nanoparticles onto exfoliated graphite oxide sheets. *J. Mater. Chem.* **2008**, *18*, 5625–5629. [[CrossRef](#)]
37. Wu, L.X.; Yu, L.; Ding, X.X.; Li, P.W.; Dai, X.H.; Chen, X.M.; Zhou, H.Y.; Bai, Y.Z.; Ding, J. Magnetic solid-phase extraction based on graphene oxide for the determination of lignans in sesame oil. *Food Chem.* **2017**, *217*, 320–325. [[CrossRef](#)]
38. Chang, Q.; Huang, J.; Ding, Y.; Tang, H. Catalytic Oxidation of Phenol and 2,4 Dichlorophenol by Using Horseradish Peroxidase Immobilized on Graphene Oxide/Fe₃O₄. *Molecules* **2016**, *21*, 1044. [[CrossRef](#)]
39. Ozyilmaz, G. The effect of spacer arm on hydrolytic and synthetic activity of *Candida rugosa* lipase immobilized on silica gel. *J. Mol. Catal. B Enzym.* **2009**, *56*, 231–236. [[CrossRef](#)]

40. Andre, J.; Saleh, D.; Syldatk, C.; Hausmann, R. Effect of spacer modification on enzymatic synthetic and hydrolytic activities of immobilized trypsin. *J. Mol. Catal. B Enzym.* **2016**, *125*, 88–96. [[CrossRef](#)]
41. Yamamoto, S.; Imamura, A.; Susanti, I.; Hori, K.; Tanji, Y.; Unno, H. Effect of spacer length on betalactoglobuline hydrolysis by trypsin covalently immobilized on a cellulosic support. *Food Bioprod. Process.* **2005**, *83*, 61–67. [[CrossRef](#)]
42. Rouhani, S.; Rostami, A.; Salimi, A.; Pourshiani, O. Graphene oxide/CuFe₂O₄ nanocomposite as a novel scaffold for the immobilization of laccase and its application as a recyclable nanobiocatalyst for the green synthesis of arylsulfonyl benzenediols. *Biochem. Eng. J.* **2018**, *133*, 1–11. [[CrossRef](#)]
43. Rouhani, S.; Rostami, A.; Salimi, A. Preparation and characterization of laccases immobilized on magnetic nanoparticles and their application as a recyclable nanobiocatalyst for the aerobic oxidation of alcohols in the presence of TEMPO. *RSC Adv.* **2016**, *6*, 26709–26718. [[CrossRef](#)]
44. Hummers, W.S.; Offeman, R.E. Preparation of graphitic oxide. *J. Am. Chem. Soc.* **1958**, *80*, 1339. [[CrossRef](#)]
45. Valentini, L.; Bon, S.B.; Monticelli, O.; Kenny, J.M. Deposition of amino-functionalized polyhedral oligomeric silsesquioxanes on graphene oxide sheets immobilized onto an amino-silane modified silicon surface. *J. Mater. Chem.* **2012**, *22*, 6213–6217. [[CrossRef](#)]
46. Maria-Chong, A.S.; Zhao, X.S. Functionalization of SBA-15 with APTES and Characterization of Functionalized Materials. *J. Phys. Chem. B* **2003**, *107*, 12650–12657. [[CrossRef](#)]
47. Kumar, S.; Haq, I.; Prakash, J.; Raj, A. Improved enzyme properties upon glutaraldehyde cross-linking of alginate entrapped xylanase from *Bacillus licheniformis*. *Int. J. Biol. Macromol.* **2017**, *98*, 24–33. [[CrossRef](#)]
48. Patila, M.; Kouloumpis, A.; Gournis, D.; Rudolf, P.; Stamatis, H. Laccase-Functionalized Graphene Oxide Assemblies as Efficient Nanobiocatalysts for Oxidation Reactions. *Sensors* **2016**, *16*, 287. [[CrossRef](#)]
49. Leonowicz, A.; Sarkar, J.M.; Bollag, J.M. Improvement in stability of an immobilized fungal laccase. *Appl. Microbiol. Biotechnol.* **1988**, *29*, 129–135. [[CrossRef](#)]
50. Feng, Q.; Wei, Q.; Hou, D.; Bi, S.; Wei, A.; Xu, X. Preparation of Amidoxime Polyacrylonitrile Nanofibrous Membranes and Their Applications in Enzymatic Membrane Reactor. *J. Eng. Fibers Fabr.* **2014**, *9*, 146–152. [[CrossRef](#)]
51. Bradford, M.M. A rapid and sensitive method for the quantitation of microgram quantities of protein utilizing the principle of protein-dye binding. *Anal. Biochem.* **1976**, *72*, 248–254. [[CrossRef](#)]
52. Guazzaroni, M.; Bozzini, T.; Saladino, R. Synthesis of Aldehydes by Layer-by-Layer Immobilized Laccases in the Presence of Redox Mediators. *ChemCatChem* **2012**, *4*, 1987–1996. [[CrossRef](#)]



© 2020 by the authors. Licensee MDPI, Basel, Switzerland. This article is an open access article distributed under the terms and conditions of the Creative Commons Attribution (CC BY) license (<http://creativecommons.org/licenses/by/4.0/>).